Materials Science for Energy Technologies 1 (2018) 117–128

Contents lists available at ScienceDirect

Materials Science for Energy Technologies

journal homepage: www.keaipublishing.com/en/journals/materials-science-for-energy-technologies

Transition metal oxide nanocatalysts for oxygen reduction reaction

Chiranjita Goswami [1], Kumar Kashyap Hazarika [1], Pankaj Bharali *

Department of Chemical Sciences, Tezpur University, Napaam 784 028, Assam, India

ARTICLE INFO

Article history:
Received 9 June 2018
Revised 27 June 2018
Accepted 27 June 2018
Available online 7 July 2018

Keywords:
Fuel cells
PEMFCs
ORR
TMOs

ABSTRACT

Oxygen reduction reaction (ORR) is the most important reaction that occurs in the cathode surface of fuel cells. Its sluggish kinetics stimulated the researchers towards the development of inexpensive as well as efficient alternatives, to the precious and low abundant Pt-based catalysts. Recently, transition metal-oxide (TMO) based electrocatalysts have attracted tremendous attention as suitable electrocatalyst towards ORR due to its high activity and better stability. Other factors that promote the utilization of TMOs include low cost, high availability and the presence of variable oxidation states. Mixed transition metal oxides (MTMOs) show even better ORR performance due to their enhanced electrical conductivity as compared to that of single TMOs. This review article highlights the recent progress in the design and synthesis of TMO based electrocatalysts with various size and morphology for ORR. Special importance has been given to cobalt oxides, copper oxides, manganese oxides and iron oxides throughout the study. Moreover, the effects of using conductive materials like carbon nanotubes, carbon nanofibres, mesoporous carbon, graphene etc. have also been reviewed.

Contents

1. Introduction

A safe and sustainable future can be ensured by making new innovations and modifications to the existing energy generation and storage technologies. The best way to do this is to utilize the renewable energy sources like hydroelectric power, wind, solar etc. to produce liquid fuels (via reduction reactions and electrocatalytic water splitting) and "clean" hydrogen which can be used in transportation infrastructures [1]. Usually, fuel cells are considered to be an ideal source of energy due to their high efficiency, mild operation process, zero emission and most importantly, unlimited renewable source of reactants. The main areas of fuel cell technology include transportation, stationary and portable power [2]. Fuel cells convert the chemical energy of fuels into electrical energy similar to that of batteries. However, fuel cells do not stop working till the fuels and oxidants are continuously fed [3]. Fig. 1 shows a

* Corresponding author.
E-mail address: pankajb@tezu.ernet.in (P. Bharali).
[1] Equally contributed.

https://doi.org/10.1016/j.mset.2018.06.005

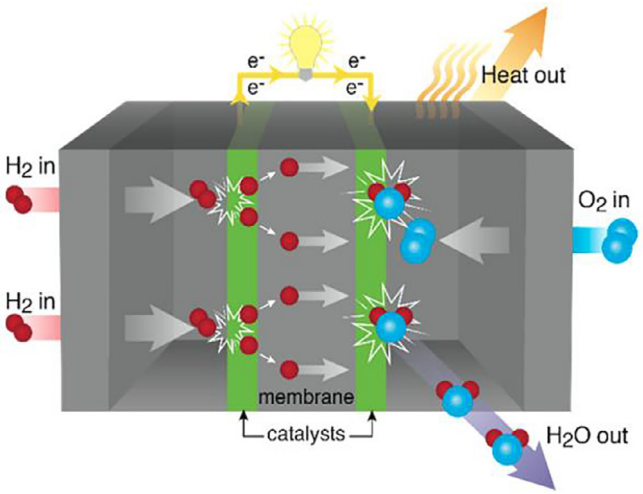

Fig. 1. A typical fuel cell. Adapted with permission from the American Chemical Society [4].

typical fuel cell in which a fuel *e.g.*; H_2 is oxidized at the anode and O_2 is reduced at the cathode [4].

Among different forms of fuel cells, proton exchange membrane fuel cells (PEMFCs) with the advantages of less ecological impact, low operating temperature and high energy density has gained a worldwide attention [5]. One of the most important reactions that take place in the cathode of the fuel cell is the oxygen reduction reaction (ORR) – a challenge in the field of catalysis and electrochemistry [6]. ORR is a multielectron transfer process that follows an electrocatalytic inner sphere mechanism. The reaction is highly dependent on the nature of the electrode surface. It takes place both in acidic and alkaline media that involves the formation of oxygen-containing intermediates like OH, O_2^-, O, H_2O_2 and HO_2^-. In aqueous medium, the reaction is highly reversible. However, the appropriate mechanisms associated with ORR have not been well understood in spite of extensive experimentation over the decades. From the point of view of electrochemistry, ORR is regarded as the kinetically limiting element of the electrochemical devices due to its sluggish kinetics [7,8]. This inspired the researchers toward the development of desirable electrocatalysts which can compensate the loss of cell efficiency by overcoming the slow kinetics of ORR [9,10]. So far, Pt and Pt-based materials have been used as the ORR electrocatalysts owing to its high electrocatalytic activity and stability, excellent work function as well as high exchange current density. However, the high price, scarcity and low durability limit its extensive commercialization [11]. In addition, the stability of Pt is low as it suffers from dissolution, agglomeration and sintering which finally results in an unusual rise in the overpotential for ORR. Thus, exploring highly abundant, low cost and durable electrocatalysts with comparable or even higher catalytic performance than that of Pt-based electrocatalysts has become a keen interest for the researchers [12–14]. One way to make PEMFCs inexpensive and durable is to incorporate Pt more in the catalyst layers. It can be done by using effective support materials (*e.g.*; carbon materials) along with Pt nanoparticles or alloying Pt with inexpensive metals like Co, Ni, Fe etc. However, this approach didn't work well on a long term basis due to ever-growing price of Pt [15,16]. So, there was a need to search for another viable solution that can persist over a long time. Thus, various efforts have been made over the past few decades to design non-precious metal based catalysts as cost effective alternatives to Pt-based catalysts for ORR [17]. Another class of material that finds wide application as electrocatalysts as well as supports is the non-noble metal oxides [18,19]. Again, both theoretical and experimental studies have revealed that transition metal-oxide (TMO) based catalysts having spinel structure act as proficient electrode material for fuel cells and other energy conversion and storage devices [20]. Mixed transition metal oxides (MTMOs), obtained from the combination of a TMO and a post-TMO or a mixture of two low priced TMOs into different spinel structures show even better electrocatalytic performance towards ORR. They also have significantly higher electrical conductivity than the simple TMOs [21]. The unique property of TMOs that facilitates better ORR performance is the presence of variable oxidation states and its ability to mix well into one material. Moreover, TMOs are commercially affordable due to its low price and high abundance which makes them very likely to be used as electrocatalysts for ORR [22]. In this review, we mainly focus on the electrocatalytic activity of TMO based catalysts with different structural properties towards ORR. We have also given a brief summary of the principle and mechanism involved in ORR. To make it feasible, the scope of this review focuses mainly on four types of TMOs namely cobalt oxides, copper oxides, manganese oxides and iron oxides.

2. General principle and mechanism of ORR

In ORR, O_2 is converted to either OH^- or H_2O based on the electrolyte (acidic or alkaline) used. ORR at the cathode surface proceeds mainly via two pathways. One is the "partial" two electron reduction pathway that results in the formation of adsorbed H_2O_2 species. And, the other is the "direct" four electron reduction or full reduction pathway. "Direct" four electron reduction pathway is more desirable for ORR than the partial reduction pathway since the reactivity of H_2O_2 is comparatively higher than that of the stability of H_2O [23,24]. The "direct" conversion of O_2 into H_2O involves a dissociative mechanism where the first step is the adsorption of O_2 on the metal/catalyst surface followed by breaking of the oxygen–oxygen bond to give adsorbed oxygen atoms. Subsequently, transfer of electrons to the adsorbed oxygen atoms in the form of hydrogen addition, yields surface bound hydroxyl groups. Further reduction and protonation of the hydroxyl group produces the H_2O molecule leaving behind the metal/catalyst surface. On the other hand, partial reduction of O_2 follows an associative mechanism in which the adsorption of O_2 on the metal surface doesn't lead to the cleavage of oxygen–oxygen. This alternative two electron reduction pathway finally generates H_2O_2 [25]. Table 1 shows the pathways of ORR in alkaline and acidic medium [5,26].

A typical ORR polarization curve is generally divided into three regions (Fig. 2) viz., kinetically controlled region, diffusion controlled region and mixed kinetic- and diffusion-controlled region. The kinetically controlled region represents that part where the rate of O_2 reduction is slow with a small increase in the current density with decreasing potential. Substantial rise in the current density is observed in the mixed kinetic- and diffusion-controlled area. In this region, acceleration of the reaction takes place with a marked drop in the potential value. In the diffusion controlled region, current density is determined by the rate at which diffusion

Table 1
ORR pathways in alkaline and acidic medium [5].

Electrolyte	Pathway	ORR
Alkaline aqueous solution	4 e^-	$O_2 + H_2O + 4e^- \rightarrow 4OH^-$
	2 e^-	$O_2 + H_2O + 2e^- \rightarrow HO_2^- + OH^-$
		$HO_2^- + H_2O + 2e^- \rightarrow 3OH^-$
Acidic aqueous solution	4 e^-	$O_2 + 4H^+ + 4e^- \rightarrow H_2O$
	2 e^-	$O_2 + 2H^+ + 2e^- \rightarrow H_2O_2$
		$H_2O_2 + 2H^+ + 2e^- \rightarrow 2\ H_2O$

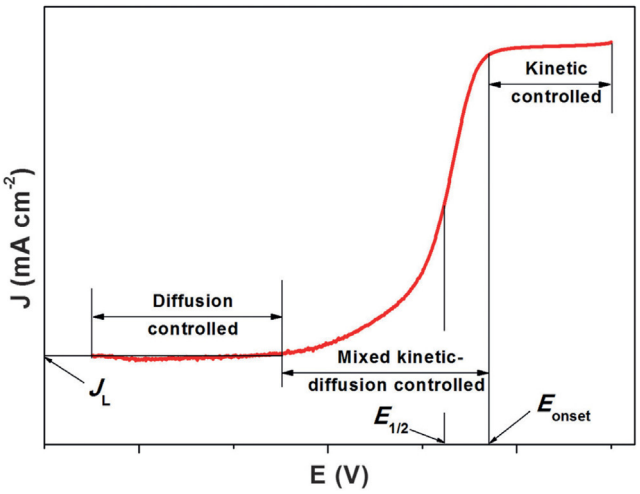

Fig. 2. A characteristic ORR curve of an individual catalyst. Adapted with permission from the Wiley publishing group [27].

of the reactants occur. Quantitative analysis of the catalyst in terms of its activity can be done from the two parameters *i.e.*; the onset potential (E_{onset}) and the half-wave potential ($E_{1/2}$). The more positive is the potential, the more active will be the catalyst towards ORR. J_L denotes the diffusion limited current density [27].

3. TMOs as nanoelectrocatalysts for ORR

As elaborated in the previous section, TMOs are prospective candidates for non-Pt ORR electrocatalysts because of the variable oxidation states combined with high electrical conductivity. This review has been focused to the application of cobalt, copper, manganese and iron oxide based electrocatalysts toward ORR.

3.1. Cobalt oxides

Cobalt oxides have been considered as the one of the promising electrode materials for fuel cell reactions, especially ORR as compared to other TMOs. Its low-price, high surface-to-volume ratio with stable chemical states and high theoretical capacity (890 mA h g^{-1}) are responsible for its application in energy related devices [28]. Co_3O_4 having spinel structure, where Co^{2+} and Co^{3+} occupy tetrahedral and octahedral voids respectively, is advantageous due to the presence of Co^{2+}/Co^{3+} redox couple where electron transfer can occur [29,30]. However, these oxides are generally stable in alkaline medium, but not in acidic medium [31,32]. Various methods like precipitation [33], thermal decomposition [34], electrodeposition [35] electrospinning [36], sol-gel [37], spray pyrolysis [38,39] etc. are employed for the synthesis of Co oxide and Co-based spinel oxides. These materials with low specific surface area and large particle size, however, undergo agglomeration as well as suffer from poor conductivity that finally affects the activity of the catalysts. One way to enhance the efficiency of electron transfer process is to make them nanostructured and use of conductive materials like graphene, carbon nanotubes, mesoporous carbon etc. [40,41]. Graphene has been emerged as a new class of conductive material having 2D aromatic monolayered C-atoms. It shows excellent thermal, mechanical, electrical and optical properties. Apart from these, graphene based materials have very high surface area, superior chemical tolerance, high structural flexibility, high stability as well as reassembly properties which may be beneficial for the energy conversion and storage devices [42–44]. Dai's group reported that a hybrid Co_3O_4 grown on reduced graphene oxide (RGO), denoted by (Co_3O_4/rmGO) exhibits tremendous electrocatalytic behaviour towards ORR and oxygen evolution reaction (OER). The unusually high activity of the catalyst can be attributed to the synergistic effect between Co_3O_4 and graphene. They have also evaluated the effect of nitrogen doping in graphene and found that the resultant catalyst *i.e.*, Co_3O_4/N-doped graphene (Co_3O_4/N-rmGO) is superior in activity as compared to that of state-of-the-art Pt in alkaline solution (Fig. 3) [45]. The reason behind this is the synergistic effect arising from the interfacial Co–O–C and Co–N–C bond formation [46]. Moreover, addition of dopants like nitrogen, boron, phophorus etc. into graphene can modify the charge distribution and spin density of the nearby C-atoms, thereby creating more active sites for ORR. Considering this, He and co-workers reported the design of a hybrid material composed of Co_3O_4 nanocrystals and 3D nitrogen-doped graphene aerogels, represented as Co_3O_4/N-GAs, to evaluate ORR and OER. The catalyst was synthesized via one-pot hydrothermal method using low cost precursors. From the linear sweep voltammetry (LSV) measurements, it is clear that the reaction proceeds through a 4 electron reaction pathway with a very high current density and high durability [47].

Tong et al. synthesized a strongly coupled hybrid consisting CoO_x nanoparticles supported on B,N-decorated graphene, denoted by CoO_xNPs/BNG. The hybrid material enriched with oxygen vacancies and Co–N–C active sites is electrocatalytically very active towards both ORR and OER. LSV measurements show that the synthesized hybrid material has a positive onset potential of 0.950 V and a half-wave potential of 0.805 V almost comparable to that of commercial Pt/C. The number of electrons transferred during the reaction, calculated using Koutecky-Levich (K-L) equation was found to be nearly 4 in the potential range, 0.2–0.6 V. This suggests that in alkaline medium (0.1 M KOH), CoO_xNPs/BNG hybrid catalyzes the reaction via "direct" four electron pathway. Again, the cyclic voltammetry (CV) and chronoamperometry tests suggest that catalyst has very high stability. Besides these, the polarization curves measured after 6000 cycles exhibited nearly the same onset and half-wave potentials as shown initially, thereby making CoO_x-NPs/BNG a potential bifunctional electrocatalyst for ORR and OER [48]. An exceptional carbon nanotube (CNT) supported nanocactus-like structure of Co_3O_4 material (Co_3O_4/CNTs) have been reported as a bifunctional electrocatalysts for ORR and OER. The strong interaction between Co_3O_4 nanoparticles and CNTs, large surface area, good electron transfer properties and abundant active sites make Co_3O_4/CNTs an effective alternative to noble metal-based catalysts for fuel cells and water splitting reactions [49]. Yoon et al. also synthesized a CNT based Co_3O_4 composite for ORR in lithium-air (Li/air) batteries. During the charge-discharge process, a low overpotential value and a high discharge capacity was observed which signifies that the catalyst is very suitable to be used as the air electrode material in Li/air batteries [50]. Another important material which has similar structure to graphite is the graphitic carbon nitride (g-C_3N_4), which finds wide application in various electrochemical reactions including ORR. Jin's group designed a highly active and stable electrocatalyst having a core-shell structure with cobalt oxide and Co-doped g-C_3N_4 as the core and shell respectively, which is covalently supported on graphene sheets (GS). The role of g-C_3N_4 shell is to generate active sites by trapping cobalt ions whereas the GS collects the electron by covalently supporting the core-shell structure. By examining the degradation mechanism of the synthesized catalyst, it was established that the high stability of the ORR activity may be generated from the cobalt oxide core that regenerates the inactive sites by slowly releasing the cobalt ions [51]. In another study, cobalt oxide nanocrystals coated multigraphene like nanoshell supported on a 3D framework of graphene nanomeshes, abbreviated as GM-Co-B-N was synthesized by rapid pyrolysis method. The resultant

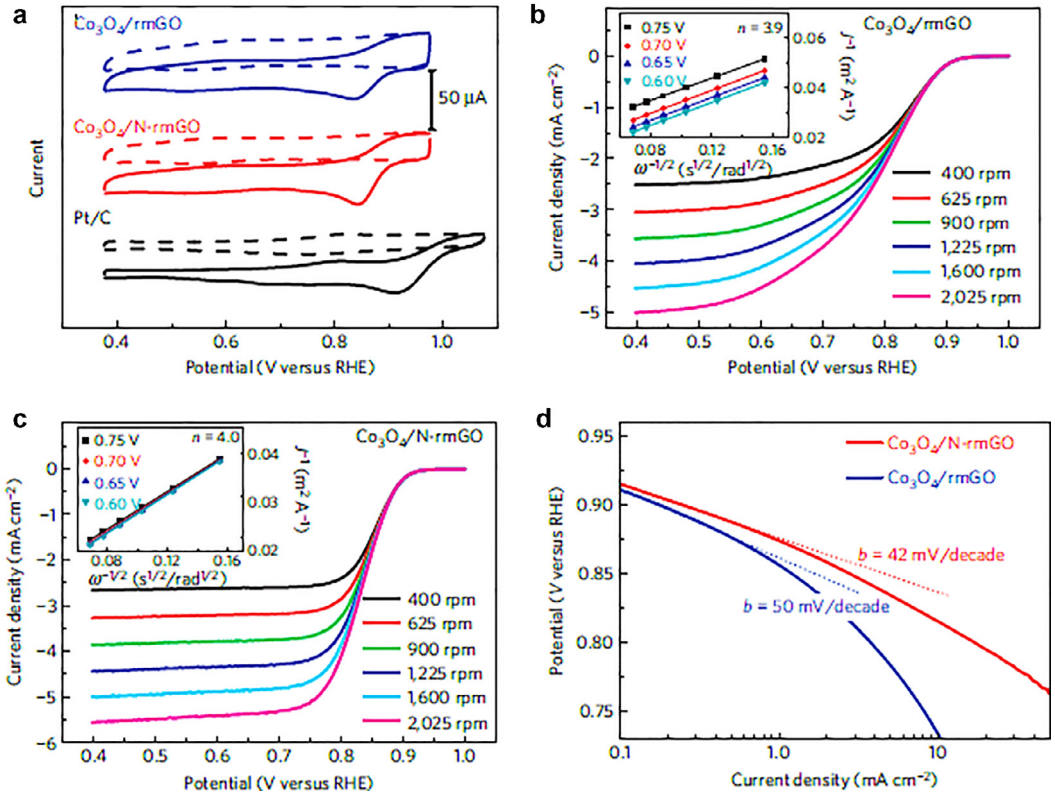

Fig. 3. (a) CV curves of Co_3O_4/N-rmGO hybrid, Co_3O_4/rmGO hybrid and comm. Pt/C on glassy carbon electrodes in Ar-saturated 0.1 M KOH (dash line) and O_2-saturated (solid line). Catalyst loading for all samples = 0.17 mg cm^{-2}. (b) ORR polarization curves of Co_3O_4/rmGO hybrid (loading ~ 0.1 mg cm^{-2}) and (c) Co_3O_4/N-rmGO hybrid (loading ~ 0.1 mg cm^{-2}) in O_2-saturated 0.1 M KOH with a sweep rate of 5 mV s^{-1} at the various rotations. Insets (b) and (c) represent Koutecky–Levich plots (J^{-1} vs. $\omega^{-0.5}$) at different potentials. (d) Tafel plots of Co_3O_4/N-rmGO and Co_3O_4/rmGO hybrids. Adapted with permission from the Nature publishing group [45].

catalyst demonstrated improved ORR and OER electrocatalytic activity, together with larger current density, similar onset/half-wave potential with commercial Pt/C, enhanced stability and strong methanol-tolerant ability, making it a promising electrocatalyst for zinc-air batteries [52]. Odedairo et al. evaluated ORR by synthesizing Co_3O_4 nanosheets as well as a novel 3D heterostructured sheet-on-sheet Co–S/G by microwave argon plasma method. This synthetic approach effectively reduces graphene oxide along with homogeneous dispersion of the Co_3O_4 nanosheets among the graphene sheets. In alkaline medium, Co–S/G exhibits the best ORR performance among all the non-precious metal electrocatalyst along with excellent durability. DFT studies shows that the charge transfer from graphene to Co_3O_4 nanosheets is the primary reason of the unusual electrocatalytic properties [53]. Ning et al. designed a highly active spinel $CuCo_2O_4$ nano-electrocatalyst supported on N-doped reduced graphene oxide ($CuCo_2O_4$/N-rGO) for ORR in alkaline medium. The good catalytic activity of $CuCo_2O_4$/N-rGO can be attributed to the strong coupling between $CuCo_2O_4$ nanoparticles and N-rGO [54]. Wu and group investigated ORR using a high loading cobalt oxide catalyst coupled to N-doped reduced graphene oxide (GO) catalyst. The resultant catalyst is abbreviated as CoO/rGO(N). The synthetic method involves the initial doping of nitrogen into reduced GO followed by incorporation of CoO. This method is better in terms of efficiency of N-doping compared to that of other methods of synthesizing N-doped reduced GO [45], in which the nitrogen source, metal precursor and GO are mixed together. Fig. 4 shows the TEM images of GO and the CoO/rGO(N) catalyst.

Fig. 4a represents the GO image where a single graphene layer is observed. The selected area electron diffraction (SAED) in the inset shows the representative hexagonal pattern of graphene. In the CoO/rGO(N) image (Fig. 4b), an area of a graphene sheet enclosed by well-dispersed nanoparticles is observed with a narrow size distribution of approximately 1–3 nm. This specifies the homogeneous loading of cobalt oxide on the rGO [55].

3.2. Copper oxides

Like cobalt oxides, copper oxides (CuO_x) also behave as a suitable non precious metal electrocatalyst for ORR due to its large surface area, variable oxidation states and chemical stability. However, the relatively poor conductivity as well as its low catalytic activity limits its widespread applications [56]. Mixing CuO_x with carbonaceous material is a highly acceptable solution to enhance its electrocatalytic properties [57]. Again, Cu^{2+} ions have a great affinity to form stable complex with N-based ligands. Thus, the combination of CuO and N-rGO gives a nanocomposite i.e., CuO/N-rGO with tremendous ORR activity. This particular nanocomposite can reduce HOO^- intermediate very rapidly resulting in high current density and more positive onset potential with a transfer of 4 electrons during the reaction. The synergic effect arising from Cu–N interaction is responsible for the improved ORR performance of the nanocomposite [58].

Nitrogen doped carbon (CN) is also used to enhance the electrical conductivity of copper oxides. A series of $NdCuO_x$@CN catalysts were synthesized by encapsulating $NdCuO_x$ bimetallic nanoparticles into CN. This piece of work amalgamates the benefits of rare-earth TMOs and CN. By optimizing the carbonization temperature and $NdCuO_x$: Aniline ratio in the precursor, the resultant catalyst $NdCuO_x$@CN-1000 was obtained. $NdCuO_x$@CN-1000 shows satisfactory ORR performance in terms of stability, activity as well as methanol tolerance. This improved ORR performance is strongly

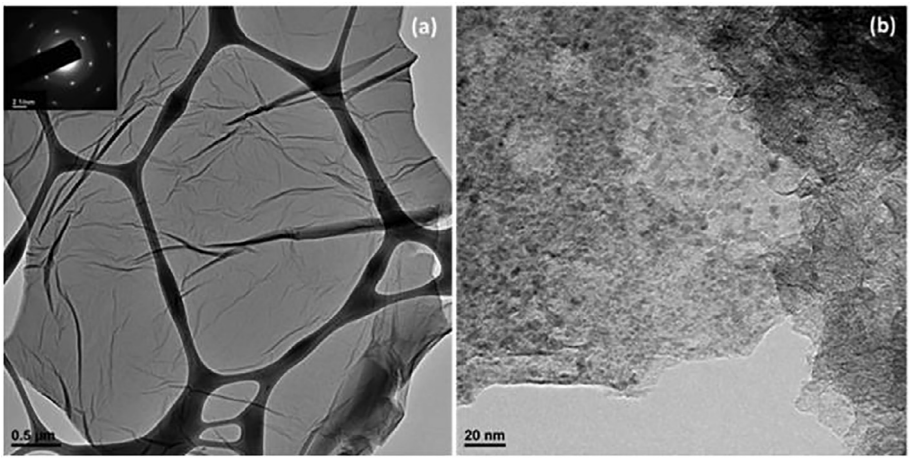

Fig. 4. TEM images (a) GO and (b) CoO/rGO(N) catalysts. Adapted with permission from the American Chemical Society [55].

associated with the synergistic effect among components, high graphitization and their encapsulated structures [59]. It is generally CuO rather than Cu_2O that is prevalent as electrocatalysts in most cases. Cu_2O easily oxidizes in wet air to give CuO, suggesting that it has the ability to donate oxygen. But, continuous supply of electrons from other materials is difficult to due to its poor conductivity. So, Cu_2O alone has no successful application as ORR catalyst. However, if Cu_2O nanoparticles with size in the nanometer scale can be homogeneously dispersed on graphene sheets, they can easily get electrons from graphene sheets after donating electrons to oxygen. Guo's group reported the synthesis of Cu_2O/rGO nanoparticles to study ORR along with its methanol and CO tolerance ability (Fig. 5). The catalyst was found to show remarkable ORR activity and stability making it a novel cathode material for

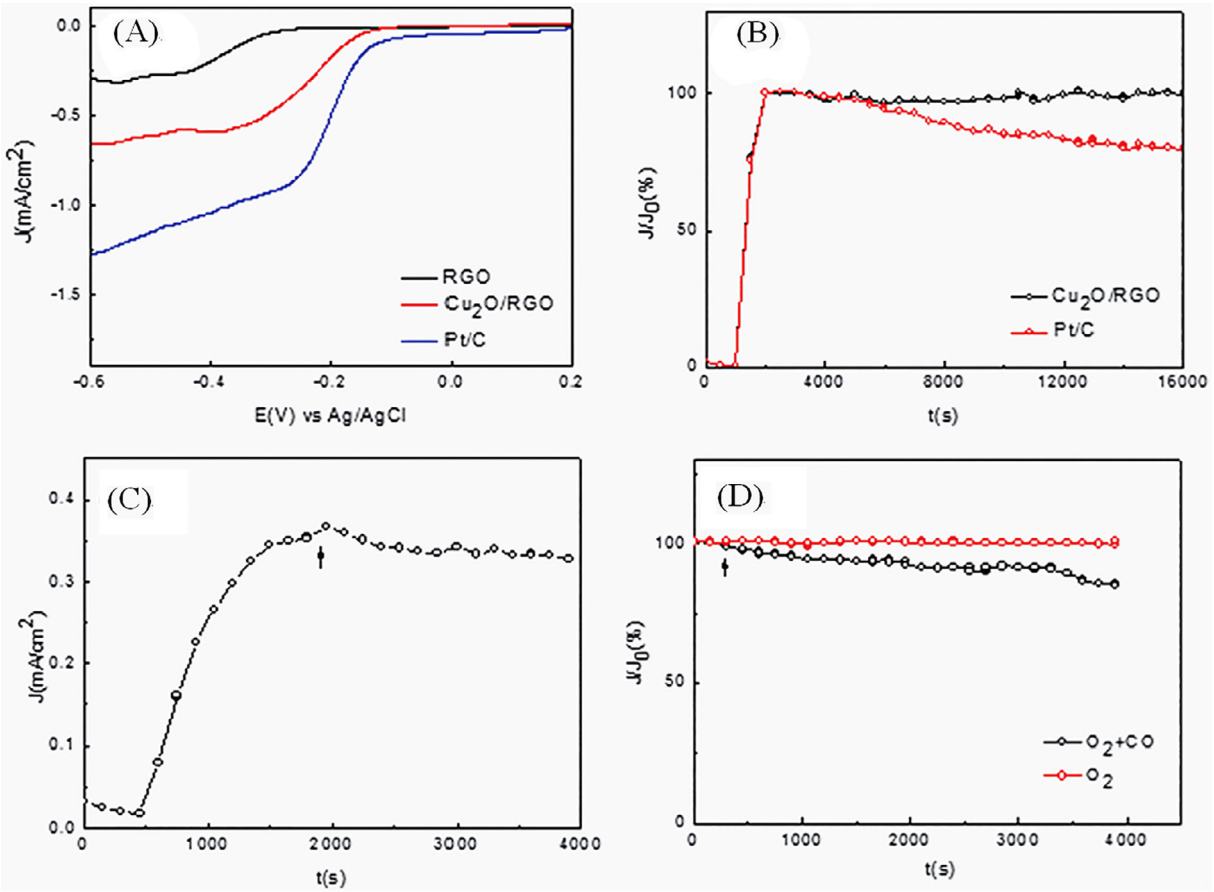

Fig. 5. ORR polarization curves of RGO and Cu_2O/RGO electrodes in O_2-saturated 0.1 M KOH solution at a scan rate of 0.01 V s^{-1}. (B) Chronoamperometric response of Cu_2O/RGO electrode and Pt/C electrode in O_2-saturated 0.1 M KOH solution at 0.4 V. (C) Chronoamperometric response of Cu_2O/RGO electrode in O_2-saturated 0.1 M KOH solution at 0.4 V. Addition of 2% (w/w) methanol is shown by the arrow. (D) Chronoamperometric response of Cu_2O/RGO electrode at −0.4 V in O_2-saturated 0.1 M KOH solution. The arrow denotes addition of 10% (v/v) CO in O_2-saturated 0.1 M KOH at −0.4 V; J_0 is the initial current. Adapted with permission from the Royal Society of Chemistry [60].

fuel cells [60]. Kim et al. synthesized Cu@Cu_2O core-shell nanocatalysts for ORR and cycloaddition reaction by sodium borohydride reduction method. The reaction follows 4-electron transfer pathway along with improved onset potential as well as current density [61]. Kim et al. designed a porous hybrid nanocomposite of CuO and graphene (p-CuO/G hybrids) for Lithium-Oxygen (Li-O_2) batteries. Electrochemical Impedence Spectroscopy (EIS) measurement shows that resultant catalyst enhances the ORR and OER activity and the cycle reversibility of Li-O_2 batteries [62]. Another study focused on the dispersion of CuO on $La_{0.6}Sr_{0.4}Co_{0.2}Fe_{0.8}O_{3-\delta}$ (LSCF) as a synergistic catalyst for ORR. LSCF is a representative solid oxide fuel cell (SOFC) electrocatalyst. The resultant catalyst greatly accelerates ORR by a factor up to 4 as obtained by the electrical conductivity relaxation measurements [63].

3.3. Manganese oxide

Transition-metal-based catalysts such as Mn oxides have attracted enormous interest due to their high stability, availability, low cost, variable oxidation states and effective catalytic properties capable of catalyzing the ORR reaction. However, due to their high electrical resistance, carbon based materials have been used to accelerate the ORR pathway [64,65]. Till now, the perovskite ($AMnO_3$) or spinel (AMn_2O_4) structure adopted by Mn-based oxides displays efficient ORR activities. Where generally A represented a divalent alkaline-earth metal ion or trivalent rare-earth metal ion, and A′ denoted a divalent metal ion. To improve the activity of Mn- based oxides oxygen defects have been introduced by thermal reduction which reduce Mn^{4+} to more active Mn^{3+}, and improve the electrical conductivity. However, the overall ORR activity of Mn-based oxides has been still higher than that of Pt/C [66]. Shao-Horn and co-workers elucidated that a mix $Mn^{3+/4+}$ valence with $Mn^{3+/4+} > 1$ was vital for the four electron ORR pathway and kinetics [67]. To design an active ORR catalyst the oxidation state of manganese centres is critical. The intermediate species for this reaction is Mn^{3+}, which plays a significant role in the success of catalytic activity in ORR. To boost the catalytic activity numerous approaches have been made to generate the active Mn^{3+} species. The high catalytic activity of the Mn^{3+} species is attributed to the presence of one electron resulting in Jahn–Teller (J–T) distortion [68]. To achieve high specific ORR activities, presence of Mn^{3+} with some Mn^{4+} is the key in perovskites [67].

Cao et al. showed that the electrochemical activity depends on the crystalline structure of manganese oxides. They show that ORR current of different MnO_2 catalysts increase in the following order: β-MnO_2 < λ-MnO_2 < γ-MnO_2 < α-MnO_2 < δ-MnO_2 [69]. Among manganese oxides targeted for ORR, Mn_3O_4 is rich in electrochemical properties due to the mixed valence of Mn. But because of its poor electrochemically structural stability and low electrical conductivity its use as ORR catalyst is diminished. Li et al. designed and constructed carbon-coated tubular monolayer superlattices (TMSLs) of hollow Mn_3O_4 NCs (h-Mn_3O_4- TMSLs) by exploiting structural evolution of MnO NCs. They have characterized the catalyst by various techniques. From Fig. 6a it can be seen that the average diameter of the particles are 18 nm. Fig. 6b, c shows the effectiveness of this in achieving high-quality nanocrystal monolayers within anodized aluminium-oxide channels. The XRD pattern of MnO@Mn_3O_4@ AAO mainly ascribed to the cubic MnO phase shown in Fig. 6d and from the XPS the presence of Mn^{2+} and Mn^{3+} can be verified shown in Fig. 6e [70].

Hazarika et al. have synthesized mesoporous cubic Mn_2O_3 nanoparticles supported on carbon (Vulcan XC 72-R) for both

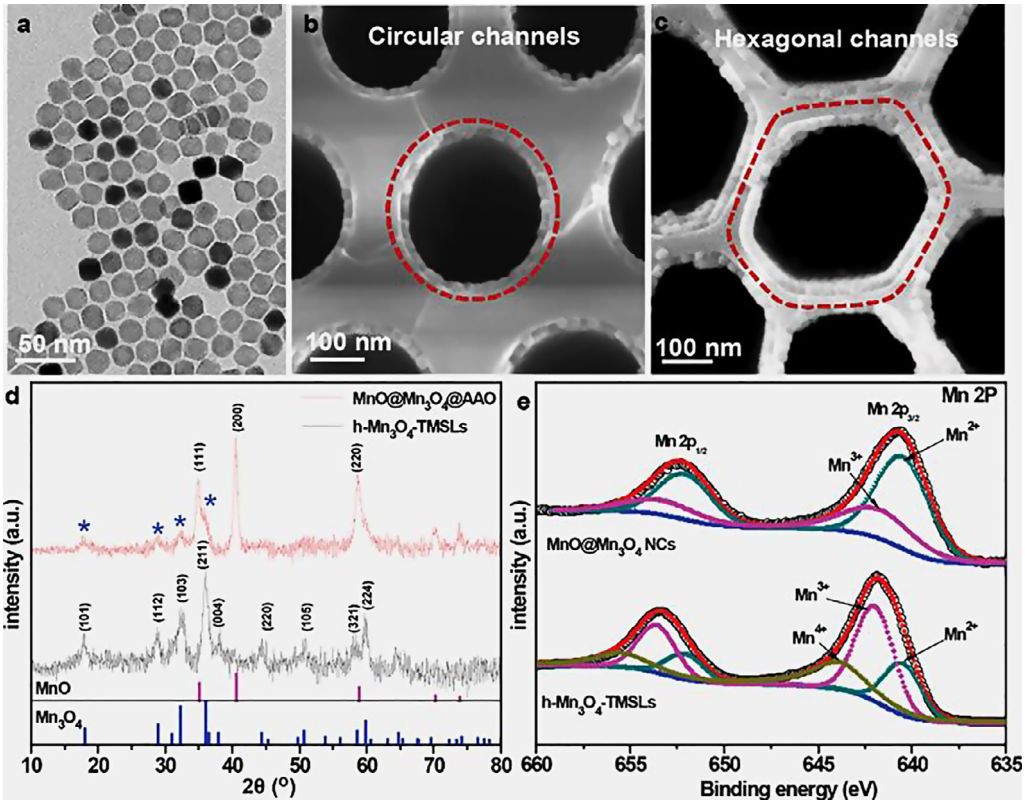

Fig. 6. (a) TEM image of octahedral MnO NCs used for constructing h-Mn_3O_4-TMSLs. Cross section SEM images of MnO NC monolayers self-assembled within the AAO template having (b) circular and (c) hexagonal channels, respectively. (d) XRD patterns of MnO@Mn_3O_4@ AAO and h-Mn_3O_4-TMSLs, respectively. The blue asterisks denote the reflections of Mn_3O_4. (e) High-resolution Mn 2p XPS spectra of MnO@Mn_3O_4 NCs and h-Mn_3O_4-TMSLs, respectively. Adapted with permission from the American Chemical Society [70].

ORR and OER. They have shown that the ORR activity of Mn_2O_3/C material is much better compared to the commercially available Pt/C and Pd/C in alkaline media. However, Mn_2O_3 without the carbon support shows less ORR activity compared to Mn_2O_3/C, Pt/C and Pd/C.

From the Fig. 7 it is seen that Mn_2O_3 is less positive and shows smaller ORR limiting current density compared to Mn_2O_3/C and both Pt/C and Pd/C catalysts and from the parallel fitting lines of the K-L plots the average electron transfer number was found to be ≈1.2 and ≈4.1 for Mn_2O_3 and Mn_2O_3/C, respectively. The high catalytic activity is due to the synergistic influence of Mn_2O_3 and carbon interface. They have also proved that Mn_2O_3/C is quite stable up to 1000 cycles and the reaction follows a 4-electron pathway for ORR [71]. Cheng et al. have reported the electrochemical properties of MnO_2-based nanostructures for ORR in alkaline media. The results show that the catalytic activity of MnO_2 follows the order α- > β- > γ-MnO_2. They have also prepared a new nanocomposite catalyst MnO_2-NWs@Ni-NPs. The as-prepared MnO_2-NWs@Ni-NPs nanocomposite exhibits an overall quasi 4-electron transfer in ORR. They have proposed the ORR mechanism for manganese oxides which are catalytically active towards peroxide decomposition. The mechanism is based on the following equations

$$MnO_2 + H_2O + e^- \leftrightarrow MnOOH + OH^- \quad (1)$$

$$2MnOOH + O_2 \leftrightarrow 2(MnOOH\cdots O) \quad (2)$$

$$MnOOH + O_2 \leftrightarrow MnOOH\cdots O_2 \quad (3)$$

$$(MnOOH\cdots O) + e^- \leftrightarrow MnO_2 + OH^- \quad (4)$$

$$MnOOH\cdots O_2 + e^- \leftrightarrow MnO_2 + HO_2^- \quad (5)$$

The total reaction of eqs 1, 2 and 4 results in an apparent 4e reduction process [13]. The combination of Mn oxide with other TMOs (such as Co, Fe, Cu oxides etc.) provides excellent ORR activity useful for a range of applications. The high catalytic activity is due to the synergistic effect of the mixed TMOs [72,73]. Li et al. have prepared ultra-small cobalt manganese spinels using simple solution-based oxidation–precipitation and insertion–crystallization process at mild condition. They have studied the catalyzation of nanocrystalline spinels for ORR. Furthermore, the strongly coupled spinel/carbon nanocomposites exhibit similar activity but superior durability to Pt/C [33]. Menezes et al. have prepared $CoMn_2O_4$ and $MnCo_2O_4$ spinel microspheres as highly efficient catalyst for OER as well as the ORR. The as-prepared cubic $MnCo_2O_4$ display better OER activity compared to the tetragonal $CoMn_2O_4$ material in an alkaline medium. However, the tetragonal $CoMn_2O_4$ material display better ORR activity and stability compared to cubic $MnCo_2O_4$ and also Pt catalysts. The structural features of the spinels and their unique porous and microspherical morphology results in the higher catalytic activity and stability of the material [74]. Liang et al. have developed a manganese-cobalt spinel $MnCo_2O_4$/graphene hybrid as a highly efficient electrocatalyst for oxygen reduction reaction (ORR) in alkaline conditions. They have suggested from the XANES of Co L-edge and Mn L-edge that substitution of Co^{3+} sites by Mn^{3+} occur resulting in higher catalytic sites in the hybrid materials enhancing the ORR activity compared to the pure cobalt oxide hybrid. They have shown that the hybrid material possess greater activity and durability than the physical mixture of nanoparticles and N-rmGO and the $MnCo_2O_4$/N-graphene hybrid displays higher ORR current density and stability compared to Pt/C in alkaline solutions at the same mass loading [32].

3.4. Iron oxide

An emerging class of TMOs like Co_xO_y, Mn_xO_y, Fe_xO_y, etc. are of considerable interest as ORR catalysts [75]. There are many advantages and disadvantages of using iron as ORR catalyst is reviewed by Osgood et al. Iron is relatively of low cost, highly abundant and has high selectivity towards ORR which makes it an alternative catalyst against the precious metals in fact iron is considered to be highly active towards ORR [76]. However, iron oxides due to their lower activity for ORR their use in fuel cells are limited [77]. Usually the unique structure and properties of the catalyst are mainly related to ORR activity [78]. But in case of iron oxides during their synthesis uncontrollable growth and agglomeration occurs which results in the decrease in their performance. To overcome these hurdles an effective approach is to use a conductive support and for that carbonized materials are very convenient. Zhao et al. have adopted a facile and solid-state low-cost method to synthesize nano-Fe_3O_4/ graphene and FeO(OH) nanoflake/graphene composites from commercially available Fe powders and graphite oxides. The prepared nano-Fe_3O_4/graphene composite displays efficient catalytic activity for both ORR and OER. They have found that the positive synergistic coupling effects between iron oxide and graphene are responsible for the observed superior properties. They have found that the ORR activity of nano-Fe_3O_4/ graphene is much higher than FeO(OH) nanoflake/graphene [79]. Zhou et al. prepared a 5-nm-thick amorphous iron oxide thin film with high electrocatalytic activity and stability. They have suggested that amorphous iron oxide can be used as the catalyst to improve oxygen reduction reaction (ORR) [77]. Also, Guo et al. from a layered tetraphenylporphyrin-based (TPP-based) covalent organic polymer (COP) as precursor and iron ion incorporation and by pyrolysis process prepared a highly active Fe_3O_4/Fe–N–C catalyst for the ORR [80]. Duchesne et al. have prepared a series of platinum–iron oxide nanoparticles by CO-reduction method. The particles formed are in the range of 3.5–4.4 nm. They have found higher activity for all three platinum–iron oxide samples nanoparticles in the ORR in comparison to a commercial Pt catalyst [81]. Zhu et al. have synthesized M(II)-substituted magnetite $M_xFe_{3-x}O_4$ ($M_xFe_{1-x}O{\cdot}Fe_2O_3$) (M = Mn, Fe, Co, Cu) nanoparticles and studied their activity for ORR in alkaline solution [82]. They have found that $M_xFe_{3-x}O_4$ NPs is the most active for the ORR followed by $Co_xFe_{3-x}O_4$, $Cu_xFe_{3-x}O_4$, and Fe_3O_4. The ORR activity of the $Mn_xFe_{3-x}O_4$ was better than the commercially available Pt catalyst. To study the electrocatalytic activity towards ORR, CV and LSV were performed. Fig. 8a shows the CVs of the C–Fe_3O_4 and C–$MnFe_2O_4$ in O_2^- saturated 0.1 M KOH aqueous solution. From the CVs it can be seen that O_2 is easily reduced on $Mn_xFe_{3-x}O_4$. Fig. 8b, c shows the ORR polarization curves of C–Fe_3O_4 and C–$MnFe_2O_4$ at different rotation rates. The K-L plots (inset of Fig. 8b, c) suggest a first order kinetics towards O_2. The number of electrons transferred was found to be ≈3.83 and ≈4.18 for Fe_3O_4 and $MnFe_2O_4$ respectively.

They have also checked the stability of the catalyst by chronoamperometric test and found better stability than the commercially available Pt catalyst [82]. Gong et al. have prepared Co[Co,Fe]O_4/ nitrogen-doped graphene (NG) composite for rechargeable Li–O_2 batteries and found better ORR activity due to the inverse spinel structure of Co[Co,Fe]O_4 and better conductivity of N-doped graphene [83]. Indra et al. have prepared amorphous and crystalline cobalt iron oxides by solvothermal method and studied their catalytic activity for photochemical and electrochemical water oxidation as well as for ORR. The prepared mixed oxides show better catalytic activities than $NiFe_2O_4$, CoO and Fe_2O_3 [84]. Carbon-supported Co-Fe_3O_4 nanoparticles are prepared by Wang et al. via a two-step reduction method and studied their catalytic activity for ORR in alkaline media and in the anion exchange membrane fuel cell (AEMFC). From the ORR activity of Co-Fe_3O_4/C the

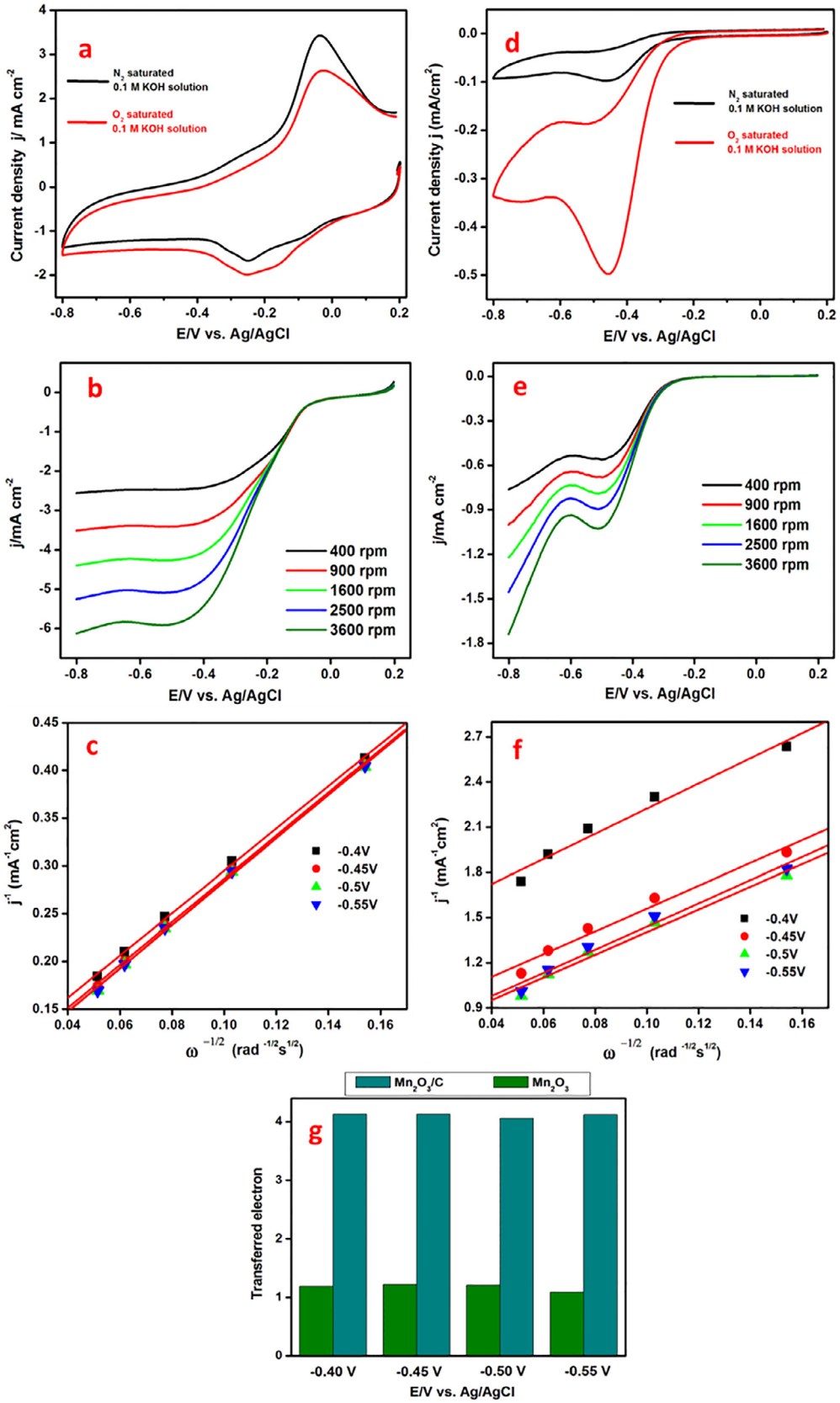

Fig. 7. (a, d) CV curves of Mn_2O_3/C and Mn_2O_3 on glassy carbon electrode in N_2 and O_2-saturated 0.1 M KOH solution; (b, e) ORR polarization curves of Mn_2O_3/C and Mn_2O_3 in O_2-saturated 0.1 M KOH solution at various rotations; (c, f) the K-L plots (j^{-1} vs. $\omega^{-1/2}$) for Mn_2O_3/C and Mn_2O_3 at different potentials; (g) Number of electron transferred at different potentials. Adapted with permission from the Elsevier [71].

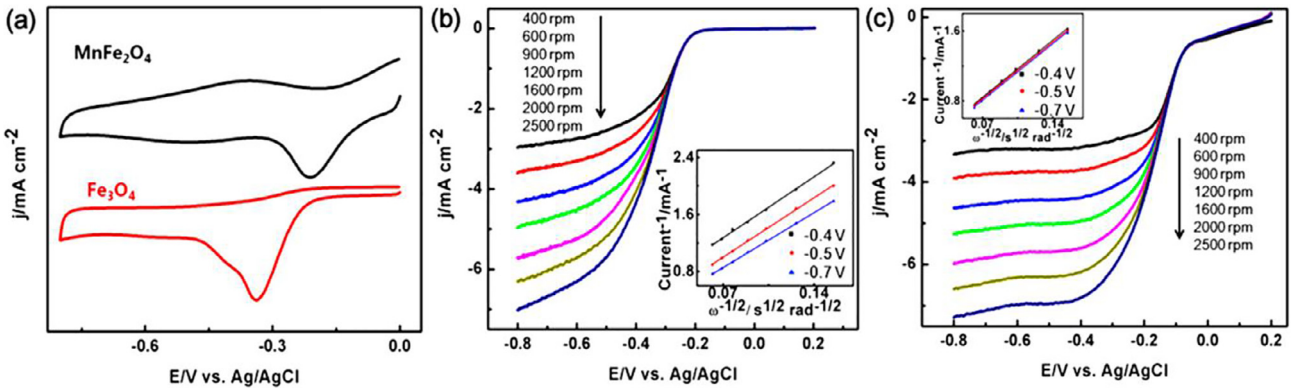

Fig. 8. (a) CV curves of C–Fe_3O_4 and C–$MnFe_2O_4$ NPs in O_2-saturated 0.1 M KOH solution (Scan rate 50 mV/s). ORR polarization curves in O_2-saturated 0.1 M KOH and at a scan rate of 10 mV/s for (b) C–Fe_3O_4 and (b) C–$MnFe_2O_4$, at different rpm (400 rpm–2500 rpm). Insets: K-L plots at different potentials (−0.4, −0.5, and −0.7 V). Adapted with permission from the American Chemical Society [82].

average electron transfer number was found to be 3.99 indicating four-electron transfer mechanism. They have compared the durability of Co-Fe_3O_4/C with Pt/C in alkaline media and found that the catalyst is more durable than Pt/C [85].

Bhandary et al. have prepared a layered binary Mn-Fe oxide on porous carbon paper via one-step electrodeposition process. They have studied the electrocatalytic activity in alkaline medium for both ORR and OER. Fig. 9a shows that the surface of the carbon paper is made of carbon rods. After electro deposition it can be seen from the Fig. 9b that Mn-Fe oxide is homogeneously grown on the surface of carbon and in Fig. 9c a nano-petal and flower like structure is seen. From the elemental analysis presented in Fig. 9d the existence of Mn, Fe and O can be evidenced. They have studied the ORR kinetics and found that the ORR process follows four-electron pathway in alkaline medium [75].

4. Summary and outlook

Research nowadays follows a trend of developing catalysts for oxygen reduction reaction which are of low cost so that it can be easily commercialized. Generally, Pt is used mainly as catalysts for ORR but due to its high cost a healthy research is going on to reduce the use of Pt in ORR. To reduce the cost and enhance the ORR performance much work has been focused on using transition metal oxides as catalysts due to their structure, exceptional electrical and redox properties which are helpful to understand their behaviour. However, despite their higher stability they suffer from poor conductivity and inferior performance compared to other current metal catalysts. So far, to increase the ORR performance various strategies are employed by mixing the transition metal oxides with other metal oxides, use of various conductive materials such

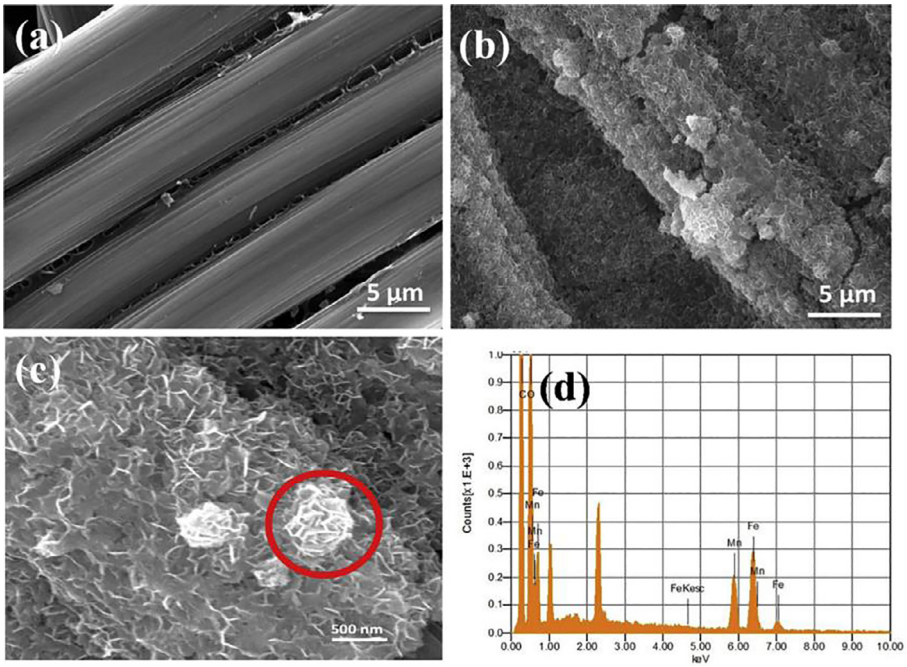

Fig. 9. SEM images of (a) carbon paper; (b) Mn-Fe oxide electro-deposited on carbon paper; (c) magnified SEM image of Mn- Fe oxide flakes shown in (b) and (d) elemental analysis of MnFe oxide. Adapted with permission from the Elsevier [75].

as carbon, metal-organic framework as supports and also by doping, the performance of ORR can be improved. The composition and the synergistic effects results in the better electro catalytic performance.

In this review, the use of transition metal oxides as an alternative ORR catalyst has been the common theme. But the mechanism of ORR at the active sites of transition metals is not fully understood yet. For cobalt oxides, the +2 oxidation state of cobalt is mainly responsible for higher ORR activity. Also, much research has been focused on cobalt and manganese mixed oxides as ORR catalyst. However, the use of ternary or complex mixed oxide as ORR catalyst is very less. Till now, many catalysts have been made that exhibits higher ORR activity but designing a catalyst with superior ORR activity and of low cost and high stability is very difficult. Various researches are going on to understand the mechanism of these oxides. By combining metal oxides with precious metals can lower the cost of the catalyst and may also provide some extra stability. It appears a bright future for electrocatalysts in ORR and noble metal free catalysts are the key to go into that future.

Acknowledgements

The authors thank Tezpur University, Council of Scientific and Industrial Research (CSIR No: 01(2813)/14/EMR-II), New Delhi and Science and Engineering Research Board (SERB-DST No: SB/FT/CS-048/2014), New Delhi for generous financial support.

References

[1] A. Kulkarni, S. Siahrostami, A. Patel, J.K. Nørskov, Understanding catalytic activity trends in the oxygen reduction reaction, Chem. Rev. 118 (2018) 2302–2312, https://doi.org/10.1021/acs.chemrev.7b00488.
[2] S. Sui, X. Wang, X. Zhou, Y. Su, S. Riffat, C. Liu, A comprehensive review of Pt electrocatalysts for the oxygen reduction reaction: nanostructure, activity, mechanism and carbon support in PEM fuel cells, J. Mater. Chem. A 5 (2017) 1808–1825, https://doi.org/10.1039/C6TA08580F.
[3] M. Shao, Q. Chang, J.-P. Dodelet, R. Chenitz, Recent advances in electrocatalysts for oxygen reduction reaction, Chem. Rev. 116 (2016) 3594–3657, https://doi.org/10.1021/acs.chemrev.5b00462.
[4] A.A. Gewirth, J.A. Varnell, A.M. Diascro, Nonprecious metal catalysts for oxygen reduction in heterogeneous aqueous systems, Chem. Rev. 118 (2018) 2313–2339, https://doi.org/10.1021/acs.chemrev.7b00335.
[5] S. Guo, S. Zhang, S. Sun, Tuning nanoparticle catalysis for the oxygen reduction reaction, Angew. Chem. Int. Ed. 52 (2013) 8526–8544, https://doi.org/10.1002/anie.201207186.
[6] A.M. Gómez-Marín, R. Rizo, J.M. Feliu, Some reflections on the understanding of the oxygen reduction reaction at Pt(111), Beilstein J. Nanotechnol. 4 (2013) 956–967, https://doi.org/10.3762/bjnano.4.108.
[7] X. Ge, A. Sumboja, D. Wuu, T. An, B. Li, F.W.T. Goh, T.S.A. Hor, Y. Zong, Z. Liu, Oxygen reduction in alkaline media: from mechanisms to recent advances of catalysts, ACS Catal. 5 (2015) 4643–4667, https://doi.org/10.1021/acscatal.5b00524.
[8] N. Ramaswamy, S. Mukerjee, Fundamental mechanistic understanding of electrocatalysis of oxygen reduction on Pt and non-Pt surfaces: acid versus alkaline media, Adv. Phys. Chem. 2012 (2012), https://doi.org/10.1155/2012/491604.
[9] H.-Q. Dong, Y.-Y. Chen, M. Han, S.-L. Li, J. Zhang, J.-S. Li, Y.-Q. Lan, Z.-H. Dai, J.-C. Bao, Synergistic effect of mesoporous Mn_2O_3-supported Pd nanoparticle catalysts for electrocatalytic oxygen reduction reaction with enhanced performance in alkaline medium, J. Mater. Chem. A 2 (2014) 1272–1276, https://doi.org/10.1039/c3ta13585c.
[10] M.K. Debe, Electrocatalyst approaches and challenges for automotive fuel cells, Nature 486 (2012) 43–51, https://doi.org/10.1038/nature11115.
[11] S. Sharma, B.G. Pollet, Support materials for PEMFC and DMFC electrocatalysts—a review, J. Power Sour. 208 (2012) 96–119, https://doi.org/10.1016/j.jpowsour.2012.02.011.
[12] K. Mohanraju, P.S. Kirankumar, L. Cindrella, O.J. Kwon, Enhanced electrocatalytic activity of Pt decorated spinals (M_3O_4, M = Mn, Fe, Co)/C for oxygen reduction reaction in PEM fuel cell and their evaluation by hydrodynamic techniques, J. Electroanal. Chem. 794 (2017) 164–174, https://doi.org/10.1016/j.jelechem.2017.04.011.
[13] F. Cheng, Y. Su, J. Liang, Z. Tao, J. Chen, MnO_2-based nanostructures as catalysts for electrochemical oxygen reduction in alkaline media, Chem. Mater. 22 (2010) 898–905, https://doi.org/10.1021/cm901698s.
[14] K. Liu, X. Huang, H. Wang, F. Li, Y. Tang, J. Li, M. Shao, Co_3O_4–CeO_2/C as a highly active electrocatalyst for oxygen reduction reaction in Al–air batteries, ACS Appl. Mater. Interfaces 8 (2016) 34422–34430, https://doi.org/10.1021/acsami.6b12294.
[15] Z. Chen, D. Higgins, A. Yu, L. Zhang, J. Zhang, A review on non-precious metal electrocatalysts for PEM fuel cells, Energy Environ. Sci. 4 (2011) 3167, https://doi.org/10.1039/c0ee00558d.
[16] R. Jiang, S. Tung, Z. Tang, L. Li, L. Ding, X. Xi, Y. Liu, L. Zhang, J. Zhang, A review of core-shell nanostructured electrocatalysts for oxygen reduction reaction, Energy Storage Mater. 12 (2018) 260–276, https://doi.org/10.1016/j.ensm.2017.11.005.
[17] X. Li, G. Liu, B.N. Popov, Activity and stability of non-precious metal catalysts for oxygen reduction in acid and alkaline electrolytes, J. Power Sour. 195 (2010) 6373–6378, https://doi.org/10.1016/j.jpowsour.2010.04.019.
[18] Z. Zhang, J. Liu, J. Gu, L. Su, L. Cheng, An overview of metal oxide materials as electrocatalysts and supports for polymer electrolyte fuel cells, Energy Environ. Sci. 7 (2014) 2535–2558, https://doi.org/10.1039/c3ee43886d.
[19] A.R. Puigdollers, P. Schlexer, S. Tosoni, G. Pacchioni, Increasing oxide reducibility: the role of metal/oxide interfaces in the formation of oxygen vacancies, ACS Catal. 7 (2017) 6493–6513, https://doi.org/10.1021/acscatal.7b01913.
[20] S. Bag, K. Roy, C.S. Gopinath, C.R. Raj, Facile single-step synthesis of nitrogen-doped reduced graphene oxide-Mn_3O_4 hybrid functional material for the electrocatalytic reduction of oxygen, ACS Appl. Mater. Interfaces 6 (2014) 2692–2699, https://doi.org/10.1021/am405213z.
[21] C. Yuan, H. Bin Wu, Y. Xie, X.W. Lou, Mixed transition-metal oxides: design, synthesis, and energy-related applications, Angew. Chem. Int. Ed. 53 (2014) 1488–1504, https://doi.org/10.1002/anie.201303971.
[22] H. Osgood, S.V. Devaguptapu, H. Xu, J. Cho, G. Wu, Transition metal (Fe Co, Ni, and Mn) oxides for oxygen reduction and evolution bifunctional catalysts in alkaline media, Nano Today 11 (2016) 601–625, https://doi.org/10.1016/j.nantod.2016.09.001.
[23] J. Stacy, Y.N. Regmi, B. Leonard, M. Fan, The recent progress and future of oxygen reduction reaction catalysis: a review, Renew. Sustain. Energy Rev. 69 (2017) 401–414, https://doi.org/10.1016/j.rser.2016.09.135.
[24] M. Shao, P. Liu, R.R. Adzic, Superoxide anion is the intermediate in the oxygen reduction reaction on platinum electrodes, J. Am. Chem. Soc. 128 (2006) 7408–7409, https://doi.org/10.1021/ja061246s.
[25] B.O.T. Holton, J.W. Stevenson, The role of platinum in proton exchange membrane fuel cells, Platinum Met. Rev. 57 (2013) 259–271, https://doi.org/10.1595/147106713X671222.
[26] Y. Zheng, Y. Jiao, M. Jaroniec, Y. Jin, S.Z. Qiao, Nanostructured metal-free electrochemical catalysts for highly efficient oxygen reduction, Small 8 (2012) 3550–3566, https://doi.org/10.1002/smll.201200861.
[27] W. Xia, A. Mahmood, Z. Liang, R. Zou, S. Guo, Earth-Abundant nanomaterials for oxygen reduction, Angew. Chem. Int. Ed. 55 (2016) 2650–2676, https://doi.org/10.1002/anie.201504830.
[28] M.M. Shahid, P. Rameshkumar, W.J. Basirun, J.C. Juan, N.M. Huang, Cobalt oxide nanocubes interleaved reduced graphene oxide as an efficient electrocatalyst for oxygen reduction reaction in alkaline medium, Electrochim. Acta 237 (2017) 61–68, https://doi.org/10.1016/j.electacta.2017.03.088.
[29] T. Zhang, C. He, F. Sun, Y. Ding, M. Wang, L. Peng, J. Wang, Y. Lin, Co_3O_4 nanoparticles anchored on nitrogen-doped reduced graphene oxide as a multifunctional catalyst for H_2O_2 reduction, oxygen reduction and evolution reaction, Sci. Rep. 7 (2017) 43638, https://doi.org/10.1038/srep43638.
[30] J. Xiao, Q. Kuang, S. Yang, F. Xiao, S. Wang, L. Guo, Surface structure dependent electrocatalytic activity of Co_3O_4 anchored on graphene sheets toward oxygen reduction reaction, Sci. Rep. 3 (2013) 2300, https://doi.org/10.1038/srep02300.
[31] M. Hamdani, R.N. Singh, P. Chartier, Co_3O_4 and Co-based spinel oxides bifunctional oxygen electrodes, Int. J. Electrochem. Sci. 5 (2010) 556–577. http://www.electrochemsci.org/papers/vol5/5040556.pdf.
[32] Y. Liang, H. Wang, J. Zhou, Y. Li, J. Wang, T. Regier, H. Dai, Covalent hybrid of spinel manganese-cobalt oxide and graphene as advanced oxygen reduction electrocatalysts, J. Am. Chem. Soc. 134 (2012) 3517–3523, https://doi.org/10.1021/ja210924t.
[33] C. Li, X. Han, F. Cheng, Y. Hu, C. Chen, J. Chen, Phase and composition controllable synthesis of cobalt manganese spinel nanoparticles towards efficient oxygen electrocatalysis, Nat. Commun. 6 (2015) 1–8, https://doi.org/10.1038/ncomms8345.
[34] L.M. Da Silva, L.A. De Faria, J.F.C. Boodts, Electrochemical impedance spectroscopic (EIS) investigation of the deactivation mechanism, surface and electrocatalytic properties of Ti/RuO_2(x)+Co_3O_4(1-x) electrodes, J. Electroanal. Chem. 532 (2002) 141–150, https://doi.org/10.1016/S0022-0728(02)00810-0.
[35] G. Wu, N. Li, D.R. Zhou, K. Mitsuo, B.Q. Xu, Anodically electrodeposited Co+Ni mixed oxide electrode: preparation and electrocatalytic activity for oxygen evolution in alkaline media, J. Solid State Chem. 177 (2004) 3682–3692, https://doi.org/10.1016/j.jssc.2004.06.027.
[36] K.N. Jung, S.M. Hwang, M.S. Park, K.J. Kim, J.G. Kim, S.X. Dou, J.H. Kim, J.W. Lee, One-dimensional manganese-cobalt oxide nanofibres as bi-functional cathode catalysts for rechargeable metal-air batteries, Sci. Rep. 5 (2015) 1–10, https://doi.org/10.1038/srep07665.
[37] N.K. Singh, J.P. Singh, R.N. Singh, Sol-gel-derived spinel Co_3O_4 films and oxygen evolution: part II. Optimization of preparation conditions and influence of the

nature of the metal salt precursor, Int. J. Hydrogen Energy 27 (2002) 895–903, https://doi.org/10.1016/S0360-3199(01)00193-8.
[38] M. Hamdani, M.I.S. Pereira, J. Douch, A. Ait Addi, Y. Berghoute, M.H. Mendonça, Physicochemical and electrocatalytic properties of Li-Co_3O_4 anodes prepared by chemical spray pyrolysis for application in alkaline water electrolysis, Electrochim. Acta 49 (2004) 1555–1563, https://doi.org/10.1016/j.electacta.2003.11.016.
[39] M.Y. Son, Y.J. Hong, Y.C. Kang, Superior electrochemical properties of Co_3O_4 yolk–shell powders with a filled core and multishells prepared by a one-pot spray pyrolysis, Chem. Commun. 49 (2013) 5678, https://doi.org/10.1039/c3cc42117a.
[40] Y. Hao, Y. Xu, J. Liu, X. Sun, Nickel–cobalt oxides supported on Co/N decorated graphene as an excellent bifunctional oxygen catalyst, J. Mater. Chem. A 5 (2017) 5594–5600, https://doi.org/10.1039/c7ta00299h.
[41] G. Xie, B. Chen, Z. Jiang, X. Niu, S. Cheng, Z. Zhen, Y. Jiang, H. Rong, Z.-J. Jiang, High catalytic activity of Co_3O_4 nanoparticles encapsulated in a graphene supported carbon matrix for oxygen reduction reaction, RSC Adv. 6 (2016) 50349–50357, https://doi.org/10.1039/c6ra09528c.
[42] G. Gnana Kumar, M. Christy, H. Jang, K.S. Nahm, Cobaltite oxide nanosheets anchored graphene nanocomposite as an efficient oxygen reduction reaction (ORR) catalyst for the application of lithium-air batteries, J. Power Sour. 288 (2015) 451–460, https://doi.org/10.1016/j.jpowsour.2015.04.029.
[43] S. Yang, G. Cui, S. Pang, Q. Cao, U. Kolb, X. Feng, J. Maier, K. Müllen, Fabrication of cobalt and cobalt oxide/graphene composites: towards high-performance anode materials for lithium ion batteries, ChemSusChem 3 (2010) 236–239, https://doi.org/10.1002/cssc.200900106.
[44] M. Yuan, Y. Yang, C. Nan, G. Sun, H. Li, S. Ma, Porous Co_3O_4 nanorods anchored on graphene nanosheets as an effective electrocatalysts for aprotic Li-O_2 batteries, Appl. Surf. Sci. 444 (2018) 312–319, https://doi.org/10.1016/j.apsusc.2018.02.267.
[45] Y. Liang, Y. Li, H. Wang, J. Zhou, J. Wang, T. Regier, H. Dai, Co_3O_4 nanocrystals on graphene as a synergistic catalyst for oxygen reduction reaction, Nat. Mater. 10 (2011) 780–786, https://doi.org/10.1038/nmat3087.
[46] H. Lu, Y. Huang, J. Yan, W. Fan, T. Liu, Nitrogen-doped graphene/carbon nanotube/ Co_3O_4 hybrids: one-step synthesis and superior electrocatalytic activity for the oxygen reduction reaction, RSC Adv. 5 (2015) 94615–94622, https://doi.org/10.1039/c5ra17759f.
[47] D. Yu, C. Xu, Y. Su, D. Liu, X. He, Nitrogen-doped graphene aerogels-supported cobaltosic oxide nanocrystals as high-performance bi-functional electrocatalysts for oxygen reduction and evolution reactions, J. Electroanal. Chem. 787 (2017) 46–54, https://doi.org/10.1016/j.jelechem.2017.01.034.
[48] Y. Tong, P. Chen, T. Zhou, K. Xu, W. Chu, C. Wu, Y. Xie, A bifunctional hybrid electrocatalyst for oxygen reduction and evolution: cobalt oxide nanoparticles strongly coupled to b, n-decorated graphene, Angew. Chem. Int. Ed. 56 (2017) 7121–7125, https://doi.org/10.1002/anie.201702430.
[49] M.S. Ahmed, B. Choi, Y.-B. Kim, Development of highly active bifunctional electrocatalyst using Co_3O_4 on carbon nanotubes for oxygen reduction and oxygen evolution, Sci. Rep. 8 (2018) 2543, https://doi.org/10.1038/s41598-018-20974-1.
[50] T.H. Yoon, Y.J. Park, Carbon nanotube/Co_3O_4 composite for air electrode of lithium-air battery, Nanoscale Res. Lett. 7 (2012) 1–11, https://doi.org/10.1186/1556-276X-7-28.
[51] J. Jin, X. Fu, Q. Liu, J. Zhang, A highly active and stable electrocatalyst for the oxygen reduction reaction based on a graphene-supported g-C_3N_4@cobalt oxide core–shell hybrid in alkaline solution, J. Mater. Chem. A 1 (2013) 10538–10545, https://doi.org/10.1039/c3ta11144j.
[52] C. Wang, Z. Zhao, X. Li, R. Yan, J. Wang, A. Li, X. Duan, J. Wang, Y. Liu, J. Wang, Three-dimensional framework of graphene nanomeshes shell/ Co_3O_4 synthesized as superior bifunctional electrocatalyst for zinc-air batteries, ACS Appl. Mater. Interfaces 9 (2017) 41273–41283, https://doi.org/10.1021/acsami.7b13290.
[53] T. Odedairo, X. Yan, J. Ma, Y. Jiao, X. Yao, A. Du, Z. Zhu, Nanosheets Co_3O_4 interleaved with graphene for highly efficient oxygen reduction, ACS Appl. Mater. Interfaces 7 (2015) 21373–21380, https://doi.org/10.1021/acsami.5b06063.
[54] R. Ning, J. Tian, A.M. Asiri, A.H. Qusti, A.O. Al-Youbi, X. Sun, Spinel $CuCo_2O_4$ nanoparticles supported on N-doped reduced graphene oxide: a highly active and stable hybrid electrocatalyst for the oxygen reduction reaction, Langmuir 29 (2013) 13146–13151, https://doi.org/10.1021/la4031014.
[55] Q. He, Q. Li, S. Khene, X. Ren, F.E. López-Suárez, D. Lozano-Castello, A. Bueno-López, G. Wu, High-loading cobalt oxide coupled with nitrogen-doped graphene for oxygen reduction in anion-exchange-membrane alkaline fuel cells, J. Phys. Chem. C 117 (2013) 8697–8707, https://doi.org/10.1021/jp401814f.
[56] Q. Hong, H. Lu, J. Wang, CuO nanoplatelets with highly dispersed Ce-doping derived from intercalated layered double hydroxides for synergistically enhanced oxygen reduction reaction in al-air batteries, ACS Sustain. Chem. Eng. 5 (2017) 9169–9175, https://doi.org/10.1021/acssuschemeng.7b02076.
[57] M. Sun, H. Liu, Y. Liu, J. Qu, J. Li, Graphene-based transition metal oxide nanocomposites for the oxygen reduction reaction, Nanoscale 7 (2015) 1250–1269, https://doi.org/10.1039/c4nr05838k.
[58] R. Zhou, Y. Zheng, D. Hulicova-Jurcakova, S.Z. Qiao, Enhanced electrochemical catalytic activity by copper oxide grown on nitrogen-doped reduced graphene oxide, J. Mater. Chem. A 1 (2013) 13179, https://doi.org/10.1039/c3ta13299d.
[59] J. Song, W. Wang, F. Wang, Y. Kang, S. Liu, Z. Lei, Encapsulated $NdCuO_x$ bimetallic nanoparticles with nitrogen doped carbon as an efficient electrocatalyst for oxygen reduction reaction, Electrochim. Acta 258 (2017) 1404–1412, https://doi.org/10.1016/j.electacta.2017.12.003.
[60] X.-Y. Yan, X.-L. Tong, Y.-F. Zhang, X.-D. Han, Y.-Y. Wang, G.-Q. Jin, Y. Qin, X.-Y. Guo, Cuprous oxide nanoparticles dispersed on reduced graphene oxide as an efficient electrocatalyst for oxygen reduction reaction, Chem. Commun. 48 (2012) 1892, https://doi.org/10.1039/c2cc17537a.
[61] A. Kim, N. Muthuchamy, C. Yoon, S. Joo, K. Park, MOF-Derived Cu@Cu_2O nanocatalyst for oxygen reduction reaction and cycloaddition reaction, Nanomaterials 8 (2018) 138, https://doi.org/10.3390/nano8030138.
[62] D.S. Kim, G.H. Lee, S. Lee, J.C. Kim, H.J. Lee, B.K. Kim, D.W. Kim, Electrocatalytic performance of CuO/graphene nanocomposites for Li–O_2 batteries, J. Alloys Compd. 707 (2017) 275–280, https://doi.org/10.1016/j.jallcom.2016.11.317.
[63] T. Hong, K. Brinkman, C. Xia, Copper oxide as a synergistic catalyst for the oxygen reduction reaction on $La_{0.6}Sr_{0.4}Co_{0.2}Fe_{0.8}O_{3-\delta}$ perovskite structured electrocatalyst, J. Power Sour. 329 (2016) 281–289, https://doi.org/10.1016/j.jpowsour.2016.08.075.
[64] A. Zhao, J. Masa, W. Xia, A. Maljusch, M.G. Willinger, G. Clavel, K. Xie, R. Schlogl, W. Schuhmann, M. Muhler, Spinel Mn-Co oxide in N-doped carbon nanotubes as a bifunctional electrocatalyst synthesized by oxidative cutting, J. Am. Chem. Soc. 136 (2014) 7551–7554, https://doi.org/10.1021/ja502532y.
[65] I. Roche, E. Chaînet, M. Chatenet, J. Vondrák, Carbon-supported manganese oxide nanoparticles as electrocatalysts for the oxygen reduction reaction (ORR) in alkaline medium: physical characterizations and ORR mechanism, J. Phys. Chem. C 111 (2007) 1434–1443, https://doi.org/10.1021/jp0647986.
[66] C. Dong, Z.W. Liu, J.Y. Liu, W.C. Wang, L. Cui, R.C. Luo, H.L. Guo, X.L. Zheng, S.Z. Qiao, X.W. Du, J. Yang, Modest oxygen-defective amorphous manganese-based nanoparticle mullite with superior overall electrocatalytic performance for oxygen reduction reaction, Small 13 (2017) 1–9, https://doi.org/10.1002/smll.201603903.
[67] K.A. Stoerzinger, M. Risch, B. Han, Y. Shao-Horn, Recent insights into manganese oxides in catalyzing oxygen reduction kinetics, ACS Catal. 5 (2015) 6021–6031, https://doi.org/10.1021/acscatal.5b01444.
[68] I.M. Mosa, S. Biswas, A.M. El-Sawy, V. Botu, C. Guild, W. Song, R. Ramprasad, J.F. Rusling, S.L. Suib, Tunable mesoporous manganese oxide for high performance oxygen reduction and evolution reactions, J. Mater. Chem. A 4 (2016) 620–631, https://doi.org/10.1039/c5ta07878d.
[69] Y.L. Cao, H.X. Yang, X.P. Ai, L.F. Xiao, The mechanism of oxygen reduction on MnO_2-catalyzed air cathode in alkaline solution, J. Electroanal. Chem. 557 (2003) 127–134, https://doi.org/10.1016/S0022-0728(03)00355-3.
[70] T. Li, B. Xue, B. Wang, G. Guo, D. Han, Y. Yan, A. Dong, Tubular monolayer superlattices of hollow Mn_3O_4 nanocrystals and their oxygen reduction activity, J. Am. Chem. Soc. 139 (2017) 12133–12136, https://doi.org/10.1021/jacs.7b06587.
[71] K.K. Hazarika, C. Goswami, H. Saikia, B.J. Borah, P. Bharali, Cubic Mn_2O_3 nanoparticles on carbon as bifunctional electrocatalyst for oxygen reduction and oxygen evolution reactions, Mol. Catal. 451 (2018) 153–160, https://doi.org/10.1016/j.mcat.2017.12.012.
[72] Z. Luo, E. Irtem, M. Ibáñez, R. Nafria, S. Martí-Sánchez, A. Genç, M. de la Mata, Y. Liu, D. Cadavid, J. Llorca, J. Arbiol, T. Andreu, J.R. Morante, A. Cabot, Mn_3O_4 @$CoMn_2O_4$–Co_xO_y nanoparticles: partial cation exchange synthesis and electrocatalytic properties toward the oxygen reduction and evolution reactions, ACS Appl. Mater. Interfaces 8 (2016) 17435–17444, https://doi.org/10.1021/acsami.6b02786.
[73] S.K. Singh, V. Kashyap, N. Manna, S.N. Bhange, R. Soni, R. Boukherroub, S. Szunerits, S. Kurungot, Efficient and durable oxygen reduction electrocatalyst based on CoMn alloy oxide nanoparticles supported over N-doped porous graphene, ACS Catal. 7 (2017) 6700–6710, https://doi.org/10.1021/acscatal.7b01983.
[74] P.W. Menezes, A. Indra, N.R. Sahraie, A. Bergmann, P. Strasser, M. Driess, Cobalt-manganese-based spinels as multifunctional materials that unify catalytic water oxidation and oxygen reduction reactions, ChemSusChem 8 (2015) 164–167, https://doi.org/10.1002/cssc.201402699.
[75] N. Bhandary, P.P. Ingole, S. Basu, Electrosynthesis of Mn-Fe oxide nanopetals on carbon paper as bi-functional electrocatalyst for oxygen reduction and oxygen evolution reaction, Int. J. Hydrogen Energy 43 (2018) 3–9, https://doi.org/10.1016/j.ijhydene.2017.12.102.
[76] Y. Ma, H. Wang, J. Key, V. Linkov, S. Ji, X. Mao, Q. Wang, R. Wang, Ultrafine iron oxide nanoparticles supported on N-doped carbon black as an oxygen reduction reaction catalyst, Int. J. Hydrogen Energy 39 (2014) 14777–14782, https://doi.org/10.1016/j.ijhydene.2014.07.108.
[77] W. Zhou, L. Ge, Z.G. Chen, F. Liang, H.Y. Xu, J. Motuzas, A. Julbe, Z. Zhu, Amorphous iron oxide decorated 3D heterostructured electrode for highly efficient oxygen reduction, Chem. Mater. 23 (2011) 4193–4198, https://doi.org/10.1021/cm201439d.
[78] M. Ma, Y. Dai, J.L. Zou, L. Wang, K. Pan, H.G. Fu, Synthesis of iron oxide/partly graphitized carbon composites as a high-efficiency and low-cost cathode catalyst for microbial fuel cells, ACS Appl. Mater. Interfaces 6 (2014) 13438–13447, https://doi.org/10.1021/am501844p.
[79] B. Zhao, Y. Zheng, F. Ye, X. Deng, X. Xu, M. Liu, Z. Shao, Multifunctional iron oxide nanoflake/graphene composites derived from mechanochemical synthesis for enhanced lithium storage and electrocatalysis, ACS Appl. Mater. Interfaces 7 (2015) 14446–14455, https://doi.org/10.1021/acsami.5b03477.
[80] J. Guo, Y. Cheng, Z. Xiang, Confined-space-assisted preparation of Fe_3O_4-nanoparticle-modified Fe–N–C catalysts derived from a covalent organic

polymer for oxygen reduction, ACS Sustain. Chem. Eng. 5 (2017) 7871–7877, https://doi.org/10.1021/acssuschemeng.7b01367.
[81] P.N. Duchesne, G. Chen, N. Zheng, P. Zhang, Local structure, electronic behavior, and electrocatalytic reactivity of CO-reduced platinum-iron oxide nanoparticles, J. Phys. Chem. C 117 (2013) 26324–26333, https://doi.org/10.1021/jp4093496.
[82] H. Zhu, S. Zhang, Y. Huang, L. Wu, S. Sun, Monodisperse M(x)Fe(3-x)O4 (M = Fe, Cu Co, Mn) nanoparticles and their electrocatalysis for oxygen reduction reaction, Nano Lett. 13 (2013) 2947–2951, https://doi.org/10.1021/nl401325u.
[83] Y. Gong, W. Ding, Z. Li, R. Su, X. Zhang, J. Wang, J. Zhou, Z. Wang, Y. Gao, S. Li, P. Guan, Z. Wei, C. Sun, Inverse spinel cobalt–iron oxide and N-doped graphene composite as an efficient and durable bifuctional catalyst for Li–O_2 batteries, ACS Catal. 8 (2018) 4082–4090, https://doi.org/10.1021/acscatal.7b04401.
[84] A. Indra, P.W. Menezes, N.R. Sahraie, A. Bergmann, C. Das, M. Tallarida, D. Schmeißer, P. Strasser, M. Driess, Unification of catalytic water oxidation and oxygen reduction reactions: amorphous beat crystalline cobalt iron oxides, J. Am. Chem. Soc. 136 (2014) 17530–17536, https://doi.org/10.1021/ja509348t.
[85] C.H. Wang, C.W. Yang, Y.C. Lin, S.T. Chang, S.L.Y. Chang, Cobalt-iron(II, III) oxide hybrid catalysis with enhanced catalytic activities for oxygen reduction in anion exchange membrane fuel cell, J. Power Sour. 277 (2015) 147–154, https://doi.org/10.1016/j.jpowsour.2014.12.007.